# Analysis of Active Space Experiments Using Artificial Relativistic Electron Beams

L. Habash Krause, B. E. Gilchrist, and T. Neubert

*Abstract*—

**An overview of several issues associated with the injection of relativistic electron beams from a satellite in Low Earth Orbit (LEO) or from a suborbital sounding rocket is presented. In particular, a model which has been developed to compute the relativistic Beam-Atmosphere Interactions (BAI) associated with the injection of relativistic electron beams (REB's) from a spacecraft has been used to characterize the dynamics of zenith-directed REB's and bremsstrahlung from nadir-directed REB's propagating in a model terrestrial upper atmosphere. It was found that choice of injection altitude of an upward propagating 5 MeV REB influences atmospheric escape energy moderately and divergence severely, consistant with the dominance of small-angle scattering in the electron BAI. The model was also used to compute downward propagating REB-induced bremsstrahlung fluxes incident on detectors on board a satellite in LEO and on a balloon, showing that the latter receives a larger bremsstrahlung dose by several orders of magnitude if the detector is oriented directly at the base of the REB propagation path.**

## I. Introduction and Background

For over two decades, spaceborne accelerators have been have been used to inject beams of energetic (1-40 keV) electrons into the terrestrial space environment to conduct active experiments in space physics and chemistry, such as magnetic field line tracing, production of artificial optical and bremsstrahlung aurora, sounding of magnetic field-aligned potential drops, and the interaction of a conducting body with the surrounding magnetized weakly-ionized gaseous environment. In support of these missions investigators had to address several technological challenges in order to ensure mission success, including experimental methods of beam propagation diagnostics and minimization of spacecraft (S/C) effects on beam particle escape from the modified environment surrounding the vehicle. Now, with the capability to potentially launch relativistic ($E \sim 5$ MeV) electron beams from a spaceborne platform in the near future [1], there is substantial interest in the investigation of these issues as they apply to beam injection in this new energy regime [2], [3], [4]. In this study we present a brief overview of some of the issues concerning active space experiments with relativistic electron beams.

Beams injected from S/C are typically of low current by laboratory standards, with the 18 A beam produced by Excede III representing the present technological upper limit of high current injection from S/C. One of the principal physical mechanisms which limit the current magnitude is the modification of the S/C potential due to the vehicle charge imbalance following particle injection. If the return current from the local plasma environment is not sufficient to balance the electron beam current, the S/C may charge to a positive potential, which may result in loss of beam energy or particle flux or in modulation of the escaping beam. Even so, results from previous experimental [5] and computational [6] studies agree that unsustained S/C charging does not necessarily impede beam propagation, especially with the implementation of charging mitigation techniques such as the release of preionized or neutral gas in the vicinity of the charged body [7], [8].

After the beam escapes the S/C sheath region, the beam interacts with the ambient environment, specifically the neutral environment (Beam-Atmosphere Interactions, BAI) and the ionized environment (Beam-Plasma Interactions, BPI). Several microphysical processes, such as ionization or bremsstrahlung emissions, may affect phenomena on a macroscopic scale, such as the modification of local conductivity along the beam's ionization trail. The conductivity modification may be large enough to allow the charge at the top of a thundercloud to discharge upwards into the ionosphere [3]. Alternatively, the beam may be used to generate energetic secondaries deep in the atmosphere in the vicinity of strong electric fields following cloud-to-ground (CG) lightning strokes. These seed electrons may be accelerated upwards and cascade into a runaway avalanche condition. That is, with judicious choice of injection parameters, it may be possible to instigate sprites or jets depending on the specific conditions of the ambient environment following CG discharges [9].

One of the primary concerns during active experiments with REB's is the method of measuring beam propagation characteristics, especially the beam energy and degree of collimation. To this end we have investigated the use of beam-generated bremsstrahlung as a potential candidate for remote sensing of the beam. Consider in the simplest case a cylindrically symetric relativistic ($E \sim 5$ MeV) electron beam propagating downward along a vertical, constant magnetic field. The magnetic field provides a focusing mechanism which constrains the beam to within its Larmor radius associated with the pitch angle of the beam particles (*e.g.*, 9.2 m for a 5 MeV beam with 0.01 radian divergence in a 0.4 G field) [10]. The beam experiences a defocusing force dominated by small-angle elastic scattering events during the early phases of propagation and inelastic events of arbitrary scattering angle during the latter portion of propagation. During the inelastic events, two processes dominate energy loss: ionization and to a lesser degree, bremsstrahlung. The relative importance of ionization and bremsstrahlung depends heavily on the energy of the beam and the propagation medium, ranging from a few percent for 5 MeV electrons to 40% for 100 MeV electrons in air [12]. Even though the fraction of energy converted to bremsstrahlung emissions is relatively small, a tremendous diagnostic benefit may be realized by capitalizing on the penetrating power of the bremsstrahlung x-rays. These x-rays are capable of penetrating deep into the Earth's atmosphere and may reach balloon altitudes, potentially providing a viable source of diagnostic radiation from which precipitating particle spectra may be inferred.

This paper presents an analysis of two of the issues associated with REB active experiments, including beam scattering and energy loss for injection upward into space and bremsstrahlung emissions which are expected to be incident on planar detectors

L. Habash Krause is with Boston College, Institute for Space Research, and is contracted to the Air Force Research Laboratory, Space Hazards Branch (VSBS), Hanscom Air Force Base, MA. E-mail: krause@plh.af.mil.

B. E. Gilchrist is with the University of Michigan, Space Physics Research Laboratory, Ann Arbor, MI. E-mail: gilchrst@eecs.umich.edu.

T. Neubert is with the Danish Meterological Institute, Solar-Terrestrial Physics Division, Copenhagen, Denmark. E-mail: neubert@dmi.min.dk.

of arbitratry position and orientation.

## II. Zenith-Directed Beam Propagation

The analytical model which is used to compute beam atmospheric propagation characteristics, such as radius, pitch angle divergence, and energy, along with a paramteric study of nadir-directed propagating REB dynamics over a wide range of injection energies (1-100 MeV), divergence values (0.01-0.1 radians), and currents (0.1-$10^4$ A) is described in detail in [2], [10]. The model is based on a set of beam envelope equations [3] which are used to track the balance of radial forces on the beam at its rms radius in the paraxial approximation. In the present study, we present new results of the analysis of zenith-directed REB dynamics.

Consider a 5 MeV, 0.1 A, 0.05 radian electron beam injected upward from a sounding rocket into the Earth's upper atmosphere. We are interested in the impact of injection altitude on beam energy and divergence as the beam escapes the collisional portion of the atmosphere. From [10], it has been determined that the altitude which represents the approximate penetration depth depth of a nadir-directed 5 MeV ($\gamma = 10.78$) beam is $\approx 42$ km. Injection altitudes were chosen above the 42 km limit: $z_i \in$ [45, 50, 60, and 90] km. The resulting beam $\gamma$ (ultimately representing beam energy normalized to $m_e c^2$) appears in Figure 1. The beam injected upward from 45 km experiences a reduction of energy to less than 40% its original value by the time it escapes the collisional atmosphere. Increasing the injection altitude naturally assists in preserving beam energy: injection altitudes of 50, 60, and 90 km result in the retention of 70%, 91%, and 100% of the beam injection energy. The beams also experience increases in the divergence values (Figure 2). The beam injected at 45 km undergoes a tremendous amount of scattering, with the beam's divergence increasing by a factor of 19 by the time it escapes the atmosphere. Higher injection altitudes of 50, 60, and 90 km result in escaping divergence values of 12, 6, and 1.2 times the injection value, respectively. Note that the influence of injection altitude on escaping beam divergence is much more severe than that on escaping beam energy. This is a natural result of the physics of light particles scattering in a medium of heavy particles: the physics is dominated by small-angle, elastic scattering processes.

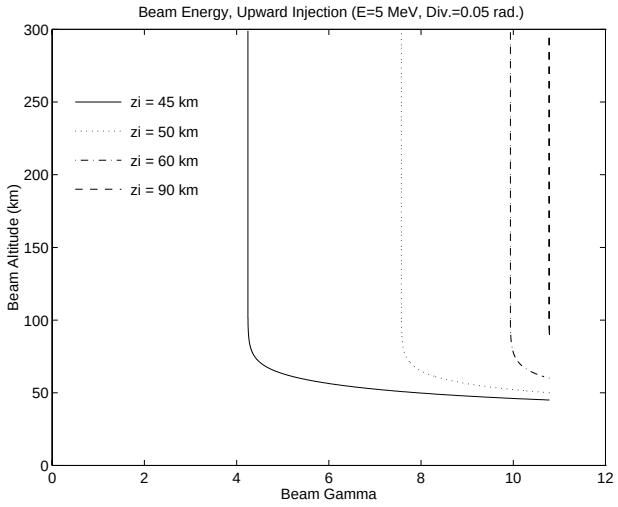


Fig. 1. Beam energy (represented by $\gamma$) as a function of altitude. 5 MeV beams are injected upward from 45, 50, 60, and 90 km.

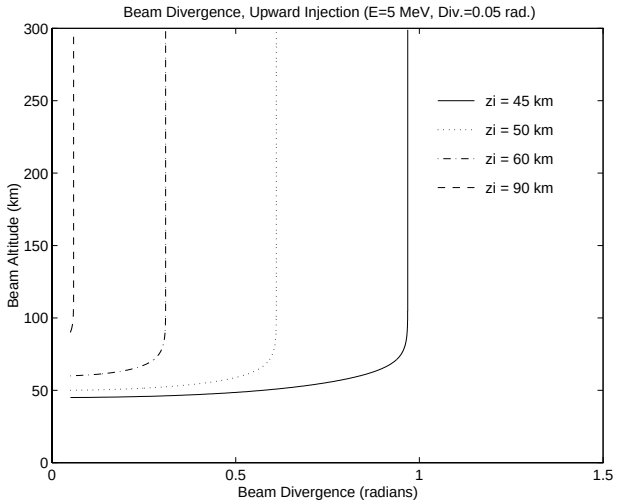


Fig. 2. Beam divergence as a function of altitude. 5 MeV beams are injected upward from 45, 50, 60, and 90 km.

## III. Bremsstrahlung Detection

The bremsstrahlung flux resulting from the slowing down of a nadir-directed 5 MeV beam in air and detected from a planar sensor on board a satellite and balloon is examined. The nature of bremsstrahlung is such that the angular distribution of the photon emission has a maximum in the forward direction and decreases rapidly with increasing emission angle (Figure 3). Thus, the bulk of the emissions will propagate in front of the beam head. We expect that as we move a detector directly behind the propagating beam, the detected emissions reach a minimum.

The bremsstrahlung is computed in the following manner: a 5 MeV beam is injected directly downward along the Earth's magnetic field. The beam brakes in the atmosphere, generating bremsstrahlung radiation along the entire path of propagation. Conversion of beam energy to bremsstrahlung is computed in the continuous loss approximation in accordance with Equation (5) from [10]. This energy is used to normalize the emissions whose distribution in emission angle and energy is represented by the Sauter cross section modified by the Elwert factor [13]. Emissions attenuated by the atmosphere propagate from the beam column to a planar detector of arbitrary position and orientation in space. Since both the bremsstrahlung production and the photon absorbtion cross section during transmission decreases with increasing photon energy, we expect a local peak in measured x-ray radiation at the detector.

First, we examine the case where the detector is on board an LEO satellite. The geometry of the system is given in Figure 4. The bremsstrahlung production column extends from the beam injection altitude ($z_{inj}$) down to the altitude of maximum penetration depth attainable by the beam ($z_{bot}$). For every source differential at the altitude $z$, there are corresponding values of:

$$\begin{aligned} \Delta z &\equiv z_{sat} - z \\ \theta_d &= \arctan(x_d/\Delta z) \\ A_{eff} &= A_d \cos\theta_d \end{aligned} \tag{1}$$

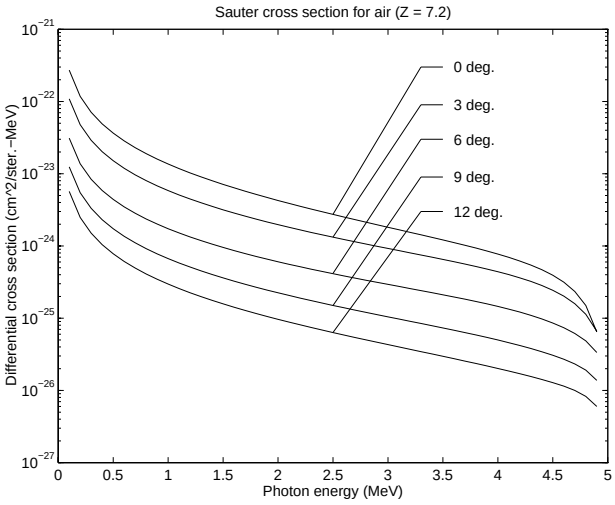


Fig. 3. Sauter cross section, differential in photon energy and emission angle, for a 5 MeV electron beam braking in air.

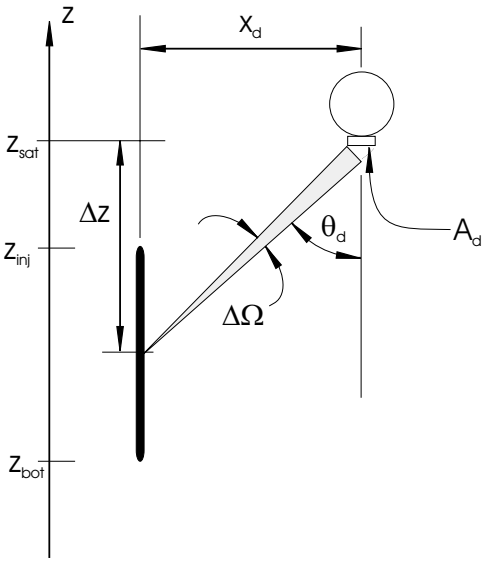


Fig. 4. Schematic of bremsstrahlung flux detection geometry, LEO altitude.

$$\Delta\Omega = \frac{A_{eff}}{(\Delta z^2 + x_d^2)}$$

where:

| | | |
|---|---|---|
| $z_{sat}$ | = | satellite altitude |
| $x_d$ | = | horizontal displacement of detector from source |
| $\theta_d$ | = | detector view angle |
| $A_d$ | = | absolute area of detector |
| $A_{eff}$ | = | effective area of detector |
| $\Delta\Omega$ | = | solid angle subtended by effective detector area |

The bremsstrahlung production rate per beam primary electron at each source altitude within $\Delta\Omega$ is:

$$P(E_{h\nu}, z)dz = n(z)\frac{d\sigma}{d\Omega}(\theta_d(z), E(z), E_{h\nu})\Delta\Omega(z)dz \qquad (2)$$

where $n(z)$ is the altitude dependent number density and $d\sigma/d\Omega$ is the Sauter-Elwert cross section as a function of $\theta_d$, beam primary energy $E$, and bremsstrahlung photon energy $E_{h\nu}$.

The bremsstrahlung flux expected to be seen by the detector, integrated over all source altitudes and attenuated by the atmosphere, is given by [14]:

$$\Psi(E_{h\nu}) = \int_{z_{inj}}^{z_{bot}} P(E_{h\nu}, z)e^{-\mu(E_{h\nu})\tau(z)}dz \qquad (3)$$

where $\mu(E_{h\nu})$ is the mass attenuation coefficient for photon propagation in air, and $\tau(z)$ is the integrated mass density along the propagation path, given by:

$$\tau(z) = \int_{z}^{z_{sat}} \frac{\rho_m(z')dz'}{\cos(\theta_d)} \qquad (4)$$

Here, $\rho_m$ is the mass density of the neutral atmosphere, assumed to be plane-stratified. The mass attenuation coefficients for radiation propagating in air were taken from [11]; these take into account the major loss processes relevant to high-energy photon transport, including the photoelectric effect, Rayleigh scattering, Compton scattering, electron-positron pair production, and photonuclear interaction.

Bremsstrahlung production is computed as a function of altitude and emission angle using the differential form of the Sauter-Elwert cross section and the results from the paraxial ray analysis of a 5 MeV beam propagating in the model atmosphere presented in [10]. The beam is injected downwards from an altitude of 240 km, and the satellite altitude is 300 km. The nadir-directed detector has an absolute area of 4.0 $m^2$. Then, the flux incident on the detector is integrated over the entire propagation length of the beam for four cases of horizontal displacement of the satellite from the beam source: $x_d \in$ [1, 10, 30, and 60] km. Since it is expected that the photons of energy less than 1 keV will be severely attenuated by the atmosphere, they were not considered in these computations. The resulting fluxes, differential in photon energy, appear in Figure 5. It is evident from this figure that larger amounts of flux are observed when the detector has a greater horizontal displacement from the radiation source. This is due to the preferential emission of bremsstrahlung in the forward direction. When the detector approaches the horizontal position almost directly overhead the beam source ($x_d = 1$ km), the bremsstrahlung intensity is at a local minimum. As the detector moves farther away from the overhead position, the intensity increases by almost two orders of magnitude when the detector is 60 km away.

Similar computations are completed for the second case in which the detector is now on a balloon at an altitude of 39 km, and the detector is oriented so that it is perpendicular to the Earth's surface and faces the base of the propagating beam. As in the LEO case, integrated bremsstrahlung was computed for four horizontal detector displacements. Since the detector is now at the base of the propagation, reducing the horizontal displacement results in increased measured bremsstrahlung flux compared with larger displacements (Figure 6).

Here, we note that, as expected, the lower energy photons experience the greatest amount of attenuation, but the fluxes have a peak at approximately 45 keV. *Berger and Seltzer* [15] found similar results with their computations of bremsstrahlung propagating in air from monoenergetic MeV beams. In the Berger and Seltzer study, omnidirectional bremsstrahlung fluxes resulting from downward-hemispherical monoenergetic electron fluxes propagating from the top of the atmosphere were computed as a function in altitude using a Monte Carlo simulation of photon transport. Compton scattering and photoelectric effect were included as scattering mechanisms. It was found that the intensity peak varied only weakly with incident electron energy;

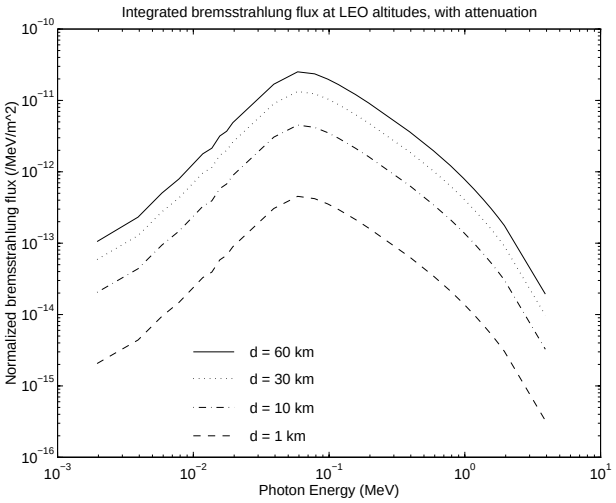


Fig. 5. Integrated bremsstrahlung flux, LEO altitude.

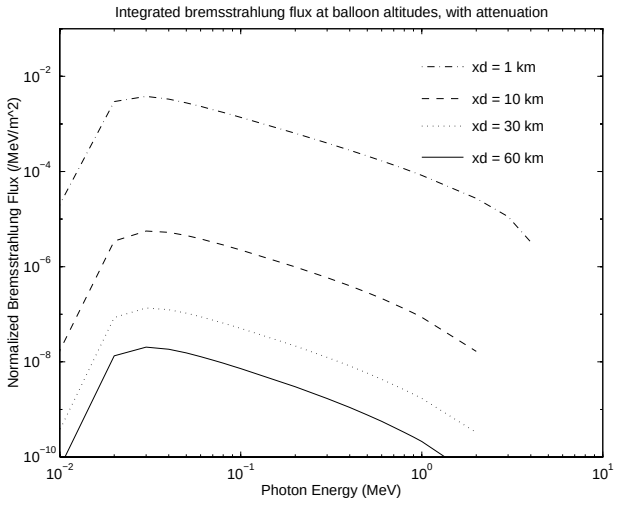


Fig. 6. Integrated bremsstrahlung flux, balloon altitude.

*i.e.,* the peak photon energy varied from approximately 35 to 45 keV for monoenergetic electrons from 50 to 2000 keV when the bremsstrahlung was measured at an altitude of $\approx$ 31 km. However, the e-folding energy of the bremsstrahlung spectra for photon energies above the peak varied strongly with incident electron energy. Thus, to use bremsstrahlung measurements as a diagnostic of precipitating electron beams energy, the photon flux e-folding energy is more useful than the peak energy.

It is also apparent that the integrated flux of attenuated bremsstrahlung is higher at the balloon detectors than it is at the satellite detectors. Thus, the optimal detection system should be one in which a detector is placed on a balloon, the balloon has a horizontal displacement sufficiently close to the beam source so that it measures a statistically significant number of photons, and the detector orientation can be manipulated to increase the effective area by aligning its normal with the line of sight of the source altitudes near the end of propagation. The orientation recommendation is important because the bulk of the bremsstrahlung production occurs in the last stages of beam propagation, and the bremsstrahlung from the higher source altitudes must traverse more of the atmosphere, and thus will be less important. If it is impractical to expect that orientation of the balloon detector can be mainpulated to point at the beam source, a satellite detector with a look direction downwards toward the Earth may be better suited to detect bremsstrahlung which may otherwise be missed if the balloon detector happens to be oriented the wrong way.

## IV. Summary

Active space experiments with relativistic electron beams present significant technological issues, some of which may be preliminarily addressed with the theoretical assessment of the Beam-Atmosphere Interactions during propagation through the collisional neutral atmosphere. In particular, it was shown that a zenith-directed relativistic electron beam has an atmospheric escape energy which decreases moderately and a divergence which increases severely when injected from an altitude near the nadir-directed penetration depth altitude. Furthermore, bremsstrahlung radiation generated by the electron beam braking in the atmosphere may be used as a remote diagnostic of the beam's characteristic energy when the photon flux e-folding energy is attainable.

## References

[1] Jost, J., Spaceborne relativistic electron accelerator system, Final Report, SBIR Program, Topic Number AF92-084, 1993.

[2] Habash Krause, L., *The Interaction of Relativistic Electron Beams with the Near-Earth Space Environment,* University of Michigan, Ph.D. Dissertation, 1998.

[3] Neubert, T., B. E. Gilchrist, S. Wilderman, L. Habash, and H. J. Wang, Relativistic Electron Beam Propagation in the Earth's Atmosphere: Modeling Results, *Geophys. Res. Lett., 23,* 1009-1012, 1996.

[4] Banks, P. M., A. C. Fraser-Smith, B. E. Gilchrist, Ionospheric modification using relativistic electron beams, *AGARD Conference Proceedings, No. 485,* pp22-1, 1990.

[5] Rappaport, S. A., R. J. Rieder, W. P. Reidy, R. L. McNutt, Jr., and J. J. Atkinson, Remote x-ray measurements of the electron beam from the EXCEDE III experiment, *J. Geophys. Res., 98,* 19093-19098, 1993.

[6] Pritchett, P. L., A three-dimensional simulation model for electron-beam injection experiments in space, *J. Geophys. Res., 96,* 13781-13793, 1991.

[7] Gilchrist, B. E., P. M. Banks, T. Neubert, P. R. Williamson, N. B. Myers, W. J. Raitt, and S. Sasaki, Electron collection enhancement arising from neutral gas jets on a charged vehicle in the ionosphere, *J. Geophys. Res, 95,* 2469-2475 , 1990

[8] Sasaki, S., N. Kawashima, K. Kuriki, M. Yanagisawa, T. Obayashi, W. T. Roberts, D. L. Reasoner, W. W. L. Taylor, P. R. Williamson, P. M. Banks, and J. L. Burch, Ignition of beam plasma discharge in the electron beam experiment in space, *Geophys. Res. Lett., 12,* 647-650, 1985

[9] Gurevich, A. V., J. A. Valdivia, G. M. Milikh, and K. Papadopoulos, Runaway electrons in the atmosphere in the presence of a magnetic field, *Radio Sci., 31*, 1541-1554, 1996.

[10] Habash Krause, L., B. E. Gilchrist, and T. Neubert, Propagation dynamics of high-altitude atmospheric relativistic electron beams, *IEEE Trans. Plasma Sci.*, submitted, 1998.

[11] Hubbell, J. H., and S. M. Seltzer, Tables of X-Ray Mass Attenuation Coefficients and Mass Energy-Absorption Coefficients from 1 keV to 20 MeV for Elements Z = 1 to 92 and 48 Additional Substances of Dosimetric Interest, *NISTIR 5632*, May 1995.

[12] Berger, M. J., and S. M. Seltzer, *Tables of energy losses and ranges of electrons and positrons,* NASA Spec. Publ. No. 3012, 1964.

[13] Koch, H. W., and J. W. Motz, Bremsstrahlung cross-section formulas and related data, *Rev. Mod. Phys., 31,* 920-955, 1959.

[14] Chamberlain, J. W., *Physics of the Aurora and Airglow,* New York, Academic Press, 1961.

[15] Berger, M. J., and S. M. Seltzer, Bremsstrahlung in the Atmosphere *J. Atmosph. Terr. Phys., 34,* 85-108, 1972.